*J. Fluid Mech.* (1994), *vol.* 261, *pp.* 33–45



# Observations of parametric instability and breaking waves in an oscillating tilted tube

By S. A. THORPE

Department of Oceanography, The University, Southampton SO9 5NH, UK

(Received 23 February 1993 and in revised form 27 May 1993)

Experiments are described in which a rectangular tube filled with a stratified fluid and tilted at an angle $\alpha$ (about 12°) is rocked at the critical frequency of waves on a slope, $\sigma = N\sin\alpha$, where $N$ is the uniform buoyancy frequency of the fluid in the central section of the tube. Localized overturns with axes transverse to the flow are observed with a scale comparable with the tube height, producing convective motions and mixing. The overturns have a periodic structure along the tube and, although occurring on each forcing cycle, they alternate in position, so that they reoccur at a given position only every two cycles, that is at the frequency of the first subharmonic of the forcing frequency. The wavelength and vertical structure of the disturbance are consistent with the presence of an internal wave mode with a frequency half that of the forcing, and this is indicative of a parametric instability. The parameters of the regions where static instability occurs show that, as observed, the fluid is more likely to be unstable to convective motions than in earlier experiments (Thorpe 1994*b*) on standing waves.

## 1. Introduction

The diapycnal transport of momentum, heat, or properties such as salinity and gas composition resulting from the breaking of internal gravity waves, is important in establishing or modifying the structure of the Earth's atmosphere and oceans. Little, however, is known about the circumstances leading to wave breaking, or of the form and nature of disturbances following the formation of regions of static instability in overturning internal gravity waves (Thorpe 1994*b*), and in consequence the identification, classification, and detection of breaking events and the parameterization of their effects, are uncertain.

An exact solution for the form of overturning progressive or standing internal waves in an infinite fluid with a uniform density gradient is available (Thorpe 1994*b*), and examples of the solution with vertical isopycnals and, at larger amplitude, with regions of static instability, are shown in figures 1(*a*) and 1(*b*), respectively. The constant phase lines are inclined to the horizontal at an angle, $\Theta$ (for clarity, in the figure chosen to be 30°), such that

$$\sigma = N\sin\Theta, \tag{1}$$

where $\sigma$ is the wave frequency. Infinitely long thin layers of statically unstable fluid are formed (stippled in figure 1*b*), lying parallel to the constant-phase lines between parallel layers in which the density gradient is greater than the mean. It is impossible to reproduce the conditions of an infinite fluid in the laboratory. It was thought, however, that some approximation both to the parallel motion along the constant phase lines and to the zero phase propagation in standing internal waves, might be possible by oscillating a tube at the frequency at which internal waves in a uniformly stratified fluid filling the tube propagate parallel to its mean slope. In particular, large

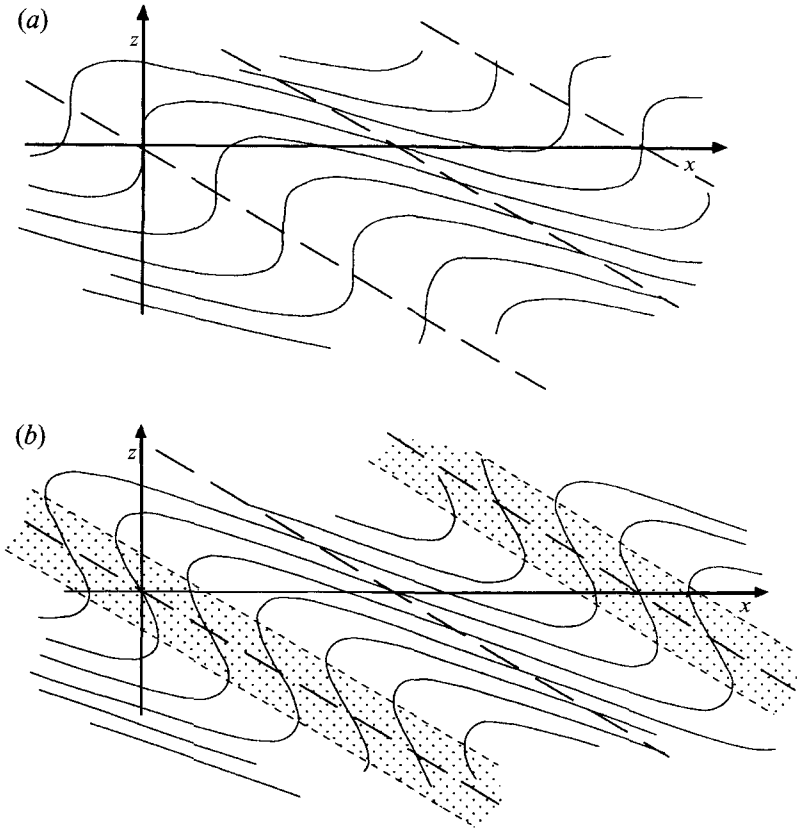


FIGURE 1. The form of isopycnal surfaces in an internal gravity wave propagating at an angle of 30° to the horizontal, (*a*) with an amplitude at which the isopycnal surfaces just become vertical; (*b*) with greater amplitude when 'overturning' occurs, with regions of static instability.

motions might be driven by increasing the oscillation amplitude. This is a description of an experiment and the observations made to test this idea. The hope of generating overturning waves like those of figure 1 was not fully realized, but other interesting phenomena were observed.

One particular process was found to dominate the developing motion. Small-amplitude internal waves in a uniform density gradient are prone to parametric instability, in which parasitic waves with frequency half that of the primary wave grow at its expense (McEwan & Robinson 1975; Mied 1976; Drazin 1977; Klostermeyer 1982, 1983). McEwan & Robinson, in particular, made a set of careful and elegant experiments in which subharmonic instability was excited in a uniformly stratified fluid contained within an oscillated cylinder, to simulate conditions occurring locally in an internal wave. They also showed that small-scale disturbances or 'traumata' noticed earlier experiments in standing waves (McEwan 1971) or resonantly interacting waves (McEwan 1973) had characteristics, particularly their orientations, consistent with their being waves resulting from a local parametric instability forced by the primary wave; since the frequency of the unstable waves is half that of the primary wave, $\sigma$, the inclination of their constant phase surfaces is given by (1) as $\sin^{-1}(\sigma/2N)$. (See also Taylor 1992 who describes further experiments on standing internal waves and small-scale turbulence.) McEwan & Robinson suggested that parametric instability should be important in the ocean, providing an effective means to cascade energy to lower

frequencies and higher wavenumbers. Mied and Drazin showed that, in inviscid fluids, even infinitesimal internal waves should be unstable, those with highest wavenumbers being the fastest growing. Mied made numerical calculations of the conditions of neutral stability and of the growth rates in inviscid fluids, finding instability for waves with $\Theta$ in the range $10° < \Theta < 80°$, but expressed the caveat that instabilities acting in concert would extract energy from the primary wave at an appreciable rate, altering its amplitude and so invalidating the assumptions of the linear theory. Klostermeyer generalized Meid's work, improving his numerical approach in the study of an inviscid Boussinesq fluid. As McEwan & Robinson showed however, knowledge of the viscous decay rate of the excited modes is necessary in order to identify which of them is unstable.

Klostermeyer (1984, 1990) has also demonstrated that parametric instability may be an important process in the atmospheric thermosphere, arguing for example that the acoustic double peaks commonly found in high-frequency Doppler spectra near thunderstorms are a consequence of the instability. The precise role of the instability in generating turbulence, the form turbulence will have and its effectiveness in mixing, however, are far from clear. Experiments are reported elsewhere (Thorpe 1994*b*) in which standing internal waves overturn and may lead to weak mixing. The experiments reported here demonstrate the severe effect that the (primary) parametric instability may have on a wave field, with the (secondary) promotion of static instability in overturning internal waves, and the subsequent (tertiary) development of convective motions and mixing.

## 2. The experiments

A tube of length $L = 2.95$ m, depth $H = 10$ cm and width $= 26$ cm, was filled in a vertical position, using the standard two-tank system with water and brine, to produce a uniform density gradient. Small quantities of dye were introduced during filling to mark isopycnal surfaces. The tube was then tilted about a horizontal axis normal to its length to an angle $\alpha$, between 11° and 14° to the horizontal. The density gradient in the tube is then uniform with constant buoyancy frequency, $N$, except in two triangular sections at the ends (see §3.1) where the gradient is diminished. The angle, $\alpha$, was chosen to be sufficiently small so that the dye layers were stretched some 4 times during the tilt, making them thin and well-defined, but $\alpha$ was sufficiently large that the central region of uniform gradient was a significant proportion of the tube length (e.g. 0.65 if $\alpha = 11°$). After the fluid had come to rest, the tube was oscillated about its inclined position through a small angle, typically 0.015 rad ($\approx 0.8°$), via a shaft linking it to an eccentric cam driven by a variable motor. The forcing frequency, $\sigma$, was chosen to be close to $N \sin \alpha$, the frequency of internal waves that have group velocities directed at an angle $\alpha$ to the horizontal. Two-dimensional waves forced at this frequency in the tube therefore propagate approximately parallel to the mean inclination of the tube or, generated away from the boundaries and later incident on the tube boundaries, are reflected as from critical slopes (Phillips 1966; Ivey & Nokes 1989).

Figure 2 shows the development of isopycnal oscillations at the centre of the tube. The isopycnal surfaces oscillate in phase with the tube, steepening as the lower end of the tube rises (figure 2*b*, *d*) and stretching (*c*, *e*) as it falls, the motion remaining in phase along the central (1.8 m) length of the tube. Except near the boundaries, the isopycnals are planar. The boundary layers near the upper and lower surfaces of the tube become turbulent after three oscillations as in the experiments on internal waves incident on critical slopes of Ivey & Nokes (1989), and the dye lines there become

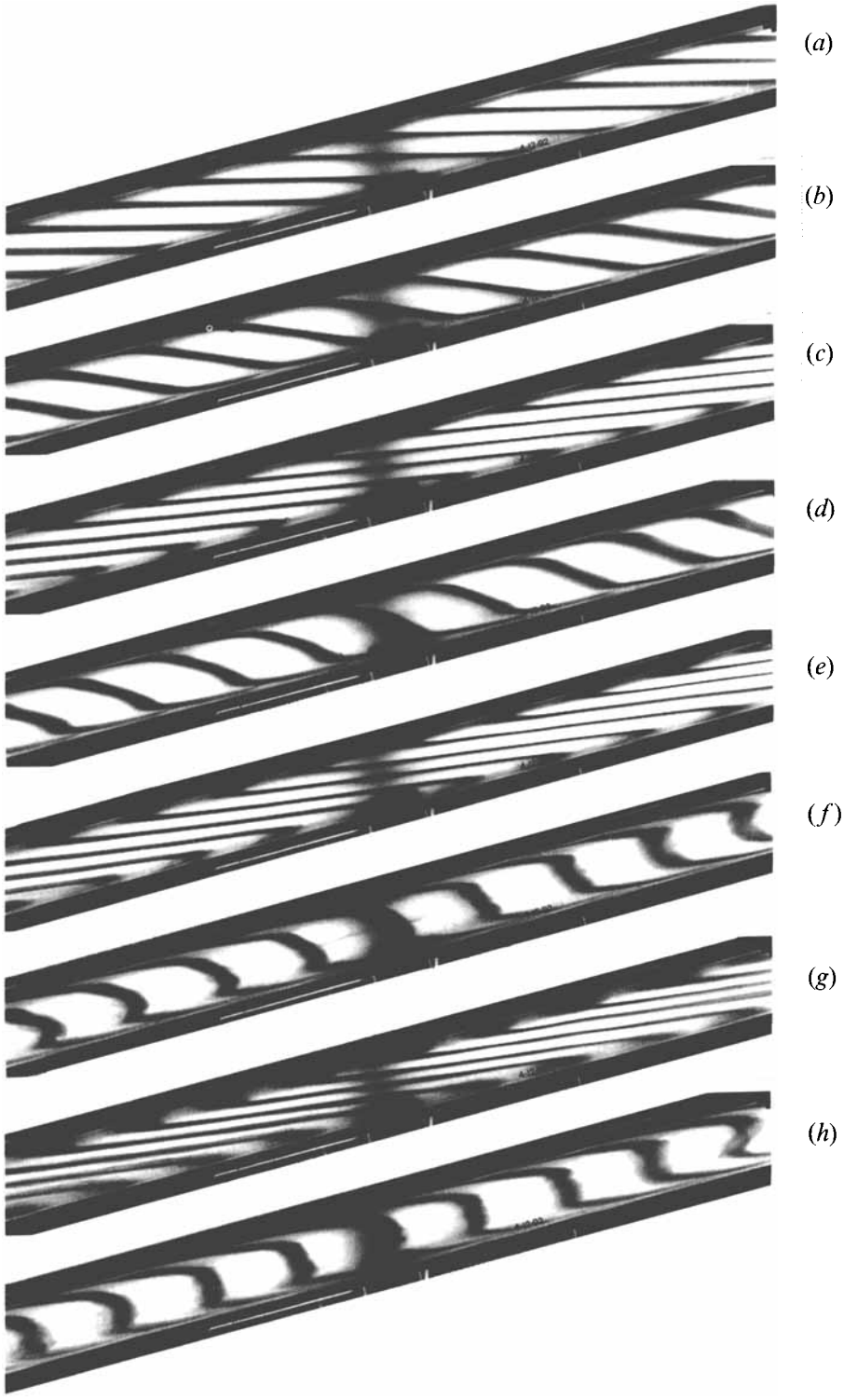


FIGURE 2. The form of dyed isopycnal surfaces in a tube inclined at an angle, $\alpha$, of 0.245 rad (14.0°) and rocked at a frequency close to that at which internal waves propagate at angle $\alpha$. Here

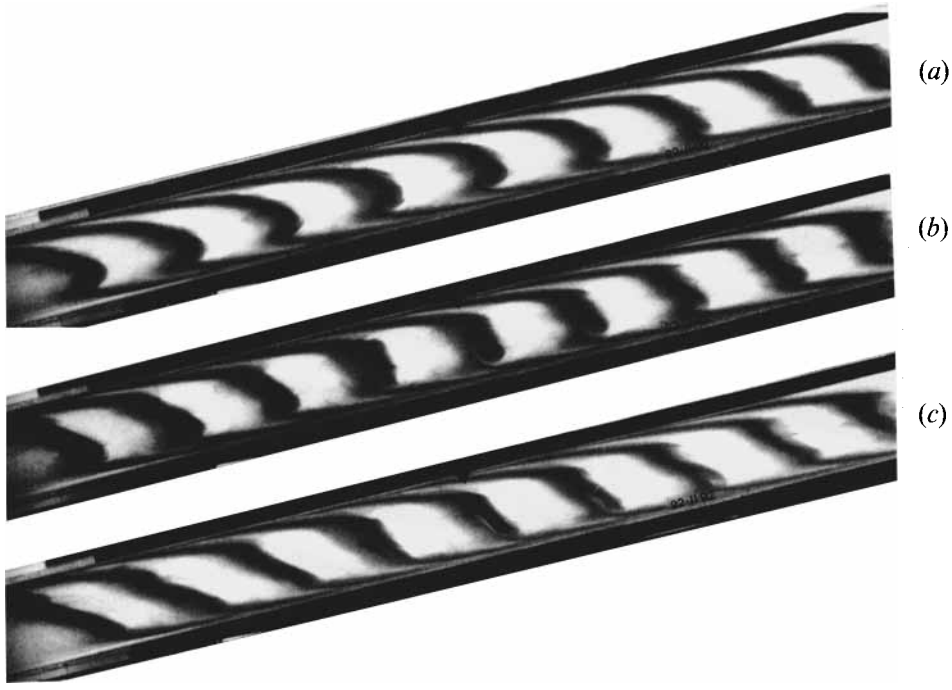


FIGURE 3. Isopycnal dyed surfaces in a rocked inclined tube – the development of overturning isopycnals. Here $\alpha = 0.192$ rad (11.0°), $N_0 = 0.501$ rad s$^{-1}$, $N = 1.114$ rad s$^{-1}$ and the critical period, $2\pi/(N \sin\alpha) = 28.69$ s. The period of the forced oscillation was 29.04 s, and the half-angle of forcing was 0.0163 rad (0.932°). The photographs were taken at 2 s intervals after 6 forcing cycles.

diffuse (figure 2*g*). The dye lines marking isopycnals eventually become almost vertical at one phase of the oscillation, with evidence of perturbations with a vertical wavenumber of about $10\pi/H$ and signs of overturning, the onset of static instability, most prominently near the upper and lower boundaries (figure 2*f*, *h*). The evolution of these overturns is shown in figure 3. The overturns appear to retain almost constant phase over lengths of 0.5–1 m along the tube. (Some of the loss of phase and resolution in the photographs is caused by parallax; the camera was about 4 m from the tube.) Figure 3(*b*, *c*) shows the onset of vertical convective motions associated with the small-scale perturbations, most clearly visible in the fourth and fifth dye bands from the right, although the photographs do not establish whether the associated motions remain two-dimensional.

Larger-scale, periodic overturn becomes apparent two cycles later. Figure 4 shows the first such large overturn to occur near the centre of the tube. Overturn is

---

$N_0 = 0.525$ rad s$^{-1}$, $N = 1.066$ rad s$^{-1}$, and the critical period, $2\pi/(N \sin\alpha) = 24.30$ s. The period of the forced oscillation was 24.24 s, and the half-angle of forcing was 0.0193 rad (1.1°). (*a*) Prior to the motion. The dye lines are horizontal, at rest. The shadow behind the centre of the tube, marked by a small triangle at the top of the tube, is caused by the tube supports. The motion begins with a downward movement of the right-hand end of the tube. Dye profiles are shown after (*b*) 2 cycles (left end rising); (*c*) $2\frac{1}{2}$ cycles (left end falling); (*d*) 3 cycles; (*e*) $3\frac{1}{2}$ cycles; (*f*) 4 cycles; (*g*) $4\frac{1}{2}$ cycles; (*h*) 5 cycles.

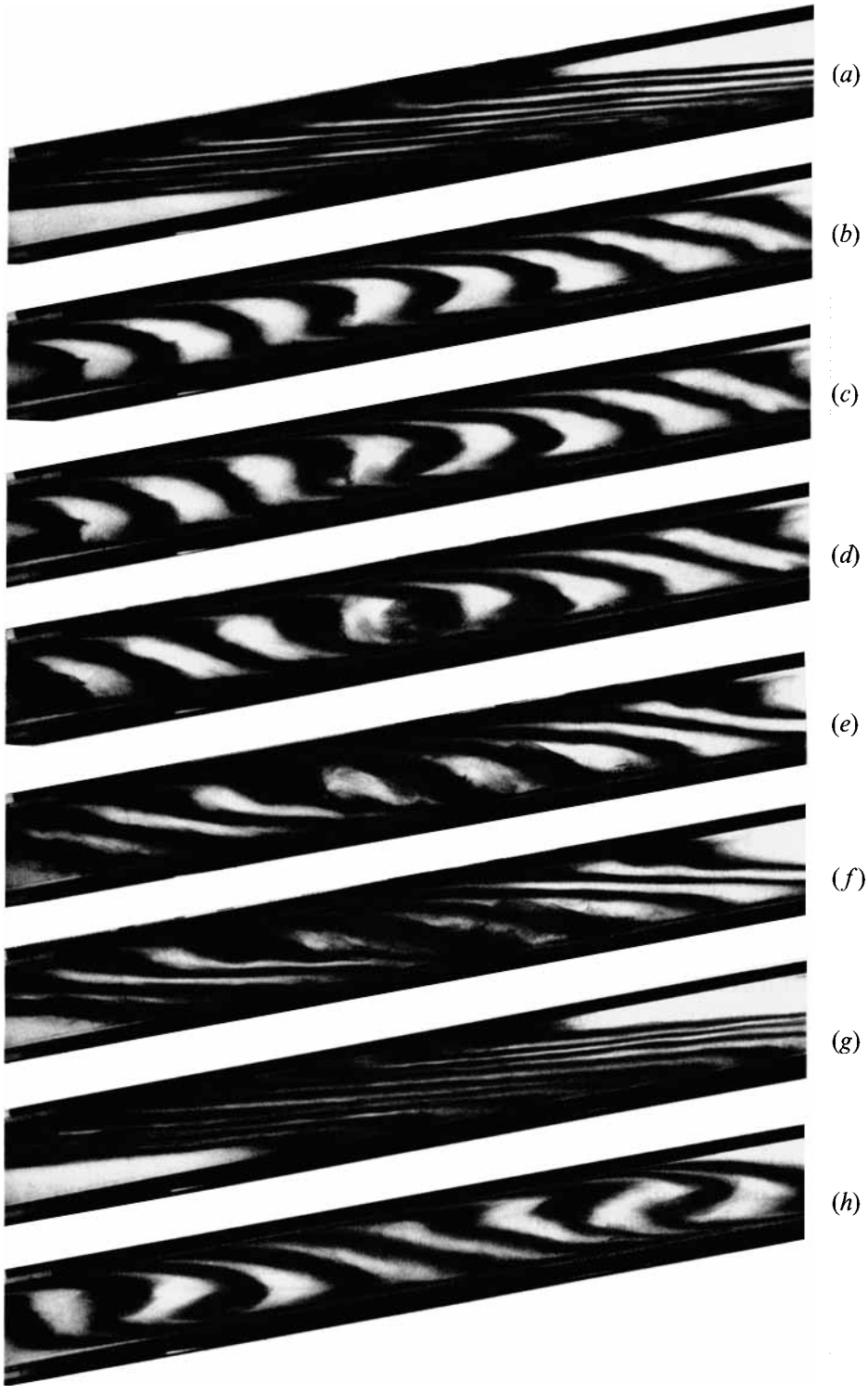


FIGURE 4. Isopycnal dyed surfaces in a rocked inclined tube – the development of overturn in the subharmonic wave; the same conditions as given in the caption of figure 3. Photographs taken after (*a*) $7\frac{1}{2}$ cycles; (*b–f*) at 2 s intervals after 8 cycles; (*g*) after $8\frac{1}{2}$ cycles; (*h*) after 9 cycles.

symmetrical in the central dye band, but occurs closer to the upper boundary to the left (lower down the slope) and nearer the lower boundary to the right, so that the shape of the 'overturning eddy' is flattened into an elliptical shape with an aspect ratio of about 0.2 and with an almost horizontal axis (figure 4*c*, *d*). The region in which the dye lines are folded, or the scale of the overturn, is about $\frac{1}{3}H$. Dye bands on either side do not overturn, but further along the tube other overturns occur in phase with that at the centre of the tube, their centres being at distances of about 60 cm (see §3.2). The overturn is followed by signs of small-scale mixing (figure 4*d–f*) before the dye lines are again stretched in the oscillating flow, as shown in figure 4(*g*), one half-period later. Figure 4(*h*), one period after figure 4(*c*), shows that no overturning occurs at the centre of the tube on the following cycle, but overturning occurs simultaneously on either side of centre in the regions where the fluid had, in figure 4(*c*), remained stably stratified. This cycle of overturning is then repeated, with overturns occurring at the centre of the tube and at locations separated by about 60 cm along the tube on either side (up to 5 occurring simultaneously) on one forcing cycle, and at intermediate positions on the next. This alternation is shown in figure 5. It continues and remains in constant phase with the forcing oscillation for at least 24 cycles, by which time the dye marking the initial isopycnals has mixed and become so diffuse that it is difficult to identify the centres of overturn.

## 3. Analysis

### 3.1. *The mean density*

The density distribution in the tilted tube can be found from the uniform gradient of density in the tube when vertical by applying the condition that the volume of fluid lying below an isopycnal must remain unchanged. Figure 6 is a sketch of the tube before and after tilt when, as in the present experiments, the tangent of the inclination angle is greater than the tube aspect ratio, $t_\alpha > H/L$. Here, and below, $s_\alpha$, $c_\alpha$, $t_{\alpha-\beta}$ etc. are equal to $\sin\alpha$, $\cos\alpha$, $\tan(\alpha-\beta)$ etc. respectively. For points at height, $z$, above the lowest point in the tube such that $0 < z < Hc_\alpha$, the volume of fluid in the triangular section below level $z$ is $z^2/(s_{2\alpha})$. This volume is equal to $yH$, where $y$ is the height in the tube, when vertical, at which is found the same density as at level $z$ in the tilted tube, so that $y = z^2/(Hs_{2\alpha})$. If the density in the tube when vertical is $\rho_0\,[1-(N_0^2/g)\,y]$, then the density in the tilted tube at height $z$ is

$$\rho(z) = \rho_0[1 - N_0^2 z^2/(gHs_{2\alpha})] \tag{2}$$

and the buoyancy frequency is $N_0\,[2z/(Hs_{2\alpha})]^{\frac{1}{2}} = n(z)$ say, tending to zero as $z$ tends to zero. The density in the tilted tube has a uniform vertical gradient when $Hc_\alpha < z < Ls_\alpha$ such that the density difference between points A and B remain the same. The vertical distance is reduced by a factor $s_\alpha$, and the vertical gradient is correspondingly increased, and the buoyancy frequency become $N_0/\sin^{\frac{1}{2}}\alpha$. The buoyancy frequency is continuous at $z = Hc_\alpha$.

### 3.2. *The forced oscillation*

McEwan & Robinson (1975) derive the equations of motion relative to an oscillating frame of reference, here that fixed in the oscillating tube. If we suppose that prior to instability the motion far from the ends of the tube is parallel to the tube walls, then the normal component is zero, and the two-dimensional continuity equation implies that the along-tube component, $u$, is independent of the along-tube coordinate, $x$. The

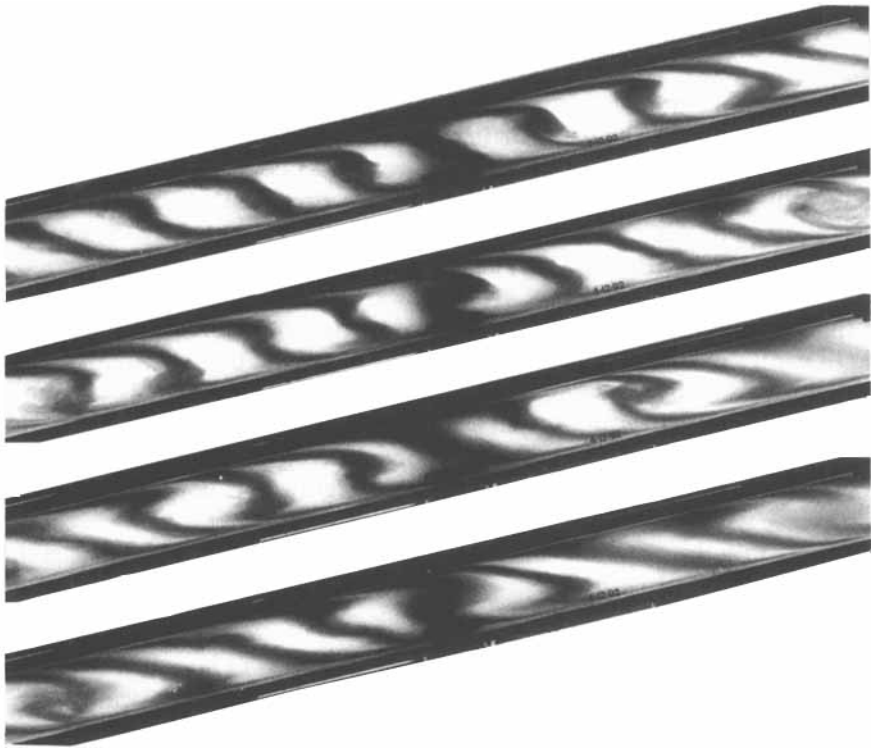


FIGURE 5. The subharmonic instability; the same conditions as given in the caption of figure 2. Photographs are at (*a*) 6; (*b*) 7; (*c*) 8; (*d*) 9 cycles after the start. The photographs (*a*) and (*c*) show no overturns at the centre, but they are apparent at either side; (*b*) and (*d*) show overturns at the centre.

nonlinear terms in the equations of motion vanish identically and, ignoring viscous terms and making the Boussinesq approximation, the equation for the along-tube momentum becomes

$$\frac{\partial^2 u}{\partial t\,\partial z} - 2\frac{\mathrm{d}^2\Omega}{\mathrm{d}t^2} = -\frac{g}{\rho_0}\frac{\partial \rho_1}{\partial z}\sin\alpha, \tag{3}$$

where $\mathrm{d}\Omega/\mathrm{d}t$ is the periodic angular velocity of the tube and $\rho_1$ is the density perturbation, given by the conservation equation

$$\frac{\partial \rho_1}{\partial t} - \frac{uN^2}{g}\rho_0 \sin\alpha = 0. \tag{4}$$

These equations combine to give

$$2\frac{\mathrm{d}^2\Omega}{\mathrm{d}t^2} - \frac{\partial^2 u}{\partial t\,\partial z} = N^2 \sin^2\alpha \frac{\partial u}{\partial z}, \tag{5}$$

which has a solution $u = f(t)\,z/H$ with $z$ measured from the mid-point of the tube, and where $f(t)$ satisfies an equation depending on time only. The depth-integrated along-tube speed is zero, satisfying the zero-net-flux condition imposed by the ends of the tube. The linear dependence of $u$ on $z$ implies that the initially plane density surfaces in the tube remain plane, as observed before the onset of instability in the experiments and away from the boundaries where viscous effects are important.

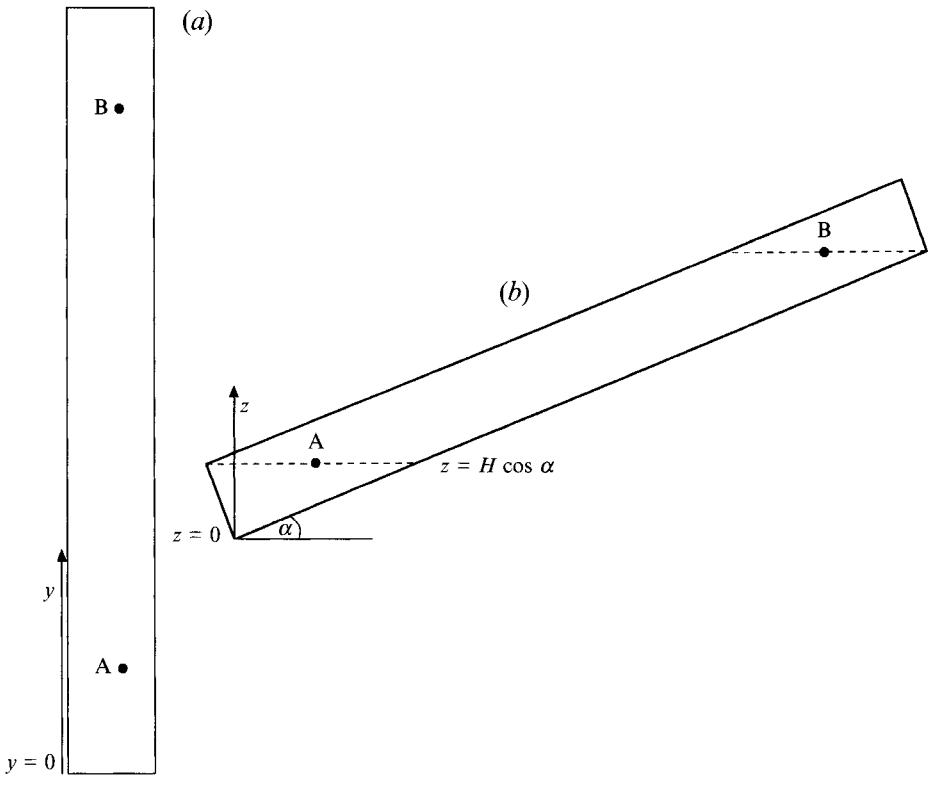


FIGURE 6. The coordinate geometry of the vertical and tilted tube.

### 3.3. *Subharmonic waves*

The inclination of the constant phase surfaces of internal waves to the horizontal is given by (1). Subharmonic waves are therefore inclined at an angle $\beta = \sin^{-1}(\sigma/2N)$ or approximately $\sin^{-1}(\frac{1}{2}\sin\alpha)$, since $\sigma/N = \sin\Theta \approx \sin\alpha$. A constant phase surface ABCDEF is sketched in figure 7. Since angles OBC and ODC are equal to $\alpha+\beta$ and $\alpha-\beta$ respectively, the along-tube wavelength, $\lambda$ = DB, is equal to $H[\cot(\alpha-\beta)-\cot(\alpha+\beta)]$, which becomes

$$\lambda = 2H(4-s_\alpha^2)^{\frac{1}{2}}/(3s_\alpha) \tag{6}$$

using the relation between $\alpha$ and $\beta$. Comparison with the distance between neighbouring overturns in the experiments, $\lambda_e$, gives, at $\alpha = 0.192$ rad (11.0°): $\lambda_e = 70 \pm 3$ cm and $\lambda = 69.4$ cm; at $\alpha = 0.203$ rad (11.6°): $\lambda_e = 60 \pm 5$ cm and $\lambda = 65.9$ cm; and at $\alpha = 0.245$ rad (14.0°): $\lambda_e = 57 \pm 2.5$ cm and $\lambda = 54.6$ cm. The estimates agree quite well with the observations.

The upper and lower corners of the tube, for example the lower corner region in $0 < z < Hc_\alpha$ (figure 6*b*), act as reflectors of incident internal waves. Perfect standing subharmonic waves will however occur only if the phase surfaces entering the corner regions are identical to those emerging. The propagation paths can be traced. Suppose that $\Phi$ is the angle of the subharmonic constant phase lines to the horizontal. Constant phase surfaces of the subharmonic waves that are incident on the bottom of the tube at an angle $\Phi$ to the horizontal that is less than the tube slope $\alpha$, are reflected as in figure 7; if the incident wave is at an acute angle to the vertical, the reflected wave is at an obtuse angle, and downward-going waves continue downwards. Now $\Phi$ is equal to

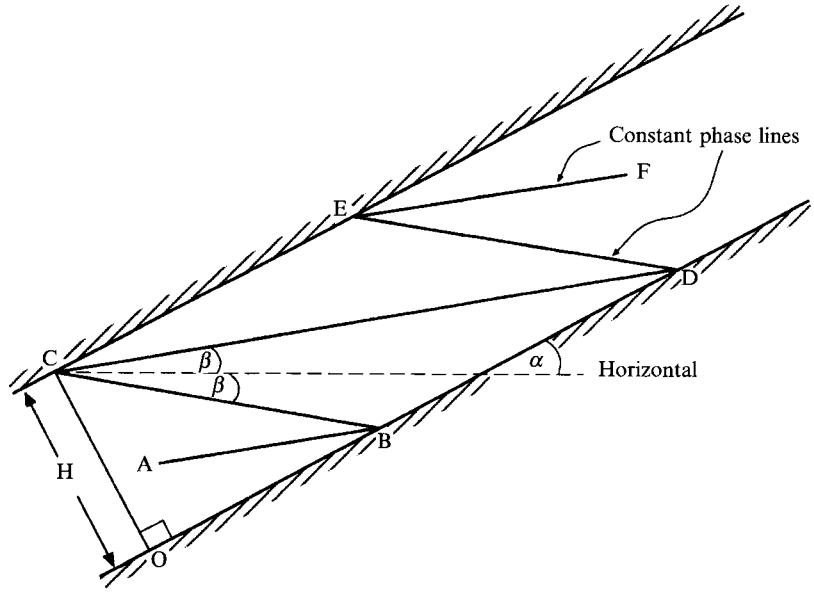


FIGURE 7. Constant phase lines of the subharmonic standing waves.

$\sin^{-1}[\sigma/2n(z)]$, which is equal to $\sin^{-1}[(\frac{1}{2}s_\alpha)(Hc_\alpha/z)^{\frac{1}{2}}]$ since $\sigma = N_0 s^{\frac{1}{2}}$. The angle $\Phi$ is therefore equal to $\alpha$ at the level $z = \frac{1}{4}Hc_\alpha$, and is equal to $\frac{1}{2}\pi$ (so the constant phase lines are vertical and reflect) at the level where $z = \frac{1}{4}Hc_\alpha s_\alpha^2$, or about 0.14 cm if $\alpha = 0.244$ rad (14°). Constant phase surfaces that meet the bottom of the tube in $\frac{1}{4}Hc_\alpha < z < Hc_\alpha$ are inclined at an angle less than $\alpha$, and reflect downwards towards the corner. When they pass below $z = \frac{1}{4}Hc_\alpha$ and meet the bottom in $\frac{1}{4}Hc_\alpha s_\alpha^2 < z < \frac{1}{4}Hc_\alpha$ however, their inclination to the horizontal exceeds $\alpha$, and they are reflected from the bottom at an acute angle to the upward vertical to re-emerge from the corner region. Perfect reflection is possible when a constant phase surface reflects in the corner at $z = \frac{1}{4}Hc_\alpha s_\alpha^2$ as sketched in figure 8. The constant phase surface is vertical at this position, its inclination to the horizontal decreasing as $z$ increases, and it first meets the lower boundary of the tube at A, figure 8, at a level $z = \frac{9}{16}Hc_\alpha^3$, reflecting back towards, and then from, the end of the tube at B to cross into the region of uniform density at C at $z = Hc_\alpha$ at a distance $x_0 = Hc_\alpha^2(32-27c_\alpha^3)/24s_\alpha$ from the end of the tube. The first reflection from the lower boundary of the tube is at D, a distance $x_1 = x_0 + H(24+27c_\alpha^4-32c_\alpha)/24t_{\alpha-\beta}$ from the lower corner. With reference to figure 8 it is seen that if $2x_1 + md - H\cot(\alpha+\beta) = L$, where $m$ is an integer and $L$ is the tube length, then perfect standing waves are possible. We have calculated the ratio

$$q = [L - 2x_1 + H\cot(\alpha+\beta)]/d$$

for the experiments. If $q$ is an integer, then an integer number of wavelengths of standing subharmonic waves can occur in the uniformly stratified section of the tube. We find that for $\alpha = 0.192$ rad, $q = 2.16 \pm 0.12$; for $\alpha = 0.203$ rad, $q = 2.39 \pm 0.12$; and for $\alpha = 0.245$ rad, $q = 3.27 \pm 0.13$. Although there is some uncertainty over these precise values because the undetermined effect of mixing during filling and tilting the tube may have altered the density structure in the corners of the tube (30% errors in the estimates of $x_0$ are indicated by the uncertainty in $q$), we conclude that it is unlikely that perfect standing subharmonic waves existed. The time for subharmonic waves to propagate along the length of the tube at their group velocity, and hence the time

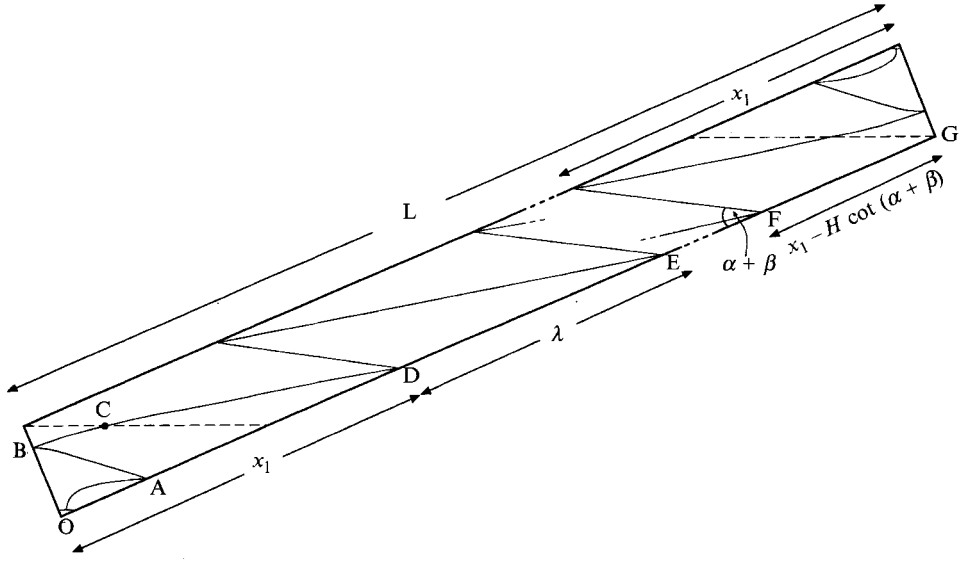


FIGURE 8. Constant phase lines for standing subharmonic waves in the tilted tube. The two end sections of the tube are sketched. The total length is $L$. The first reflection of a constant phase surface from the lower boundary of the tube, beyond the 'corner' region where the density gradient is less than in the central region of the tube, is at D. F is the first position at which the surface connecting to the upper corner of the tube reflects from the lower boundary, and F is at a distance $x_1 - H\cot(\alpha+\beta)$ from the end of the tube, G. For perfect standing wave conditions, the distance DF is an integer multiple of the wavelength, $\lambda$.

required for their establishment as normal modes, is about 330 s, or 14 cycles of the tube oscillation. We conclude that the subharmonic waves forced by the parametric instability are not normal modes of the system. We note, however, that the greatest discrepancy between the estimated wavelengths, $\lambda$, and those observed, $\lambda_e$, occurred for $\alpha = 0.203$ rad when the ratio, $q$, was furthest from an integer value, suggesting that the presence of the ends of the tube may have had some effect on the resonance.

### 3.4. *Wave overturn and mixing*

The vertical scale of the distortions to the primary forced wave seen in figures 4 and 5 suggest a mode with a vertical scale comparable with the height of the tube. The structure of the standing subharmonic wave may be determined by an extension of the theory for progressive waves reflecting from a uniform boundary. Taking coordinates $x$ and $z$ up the slope and normal to the lower boundary of the tube, respectively, the first-order density perturbations for standing waves may be written

$$\rho = \rho_1(\sigma) + \rho_1(-\sigma), \tag{7}$$

where

$$\rho(\sigma) = [N_0^2 a/(2g\sigma')]\{(kc_\alpha - n_I s_\alpha)\sin(kx + n_I z - \sigma' t) - (kc_\alpha - n_R s_\alpha)\sin(kx + n_R z - \sigma' t)\}$$

and where $a$ is proportional to the amplitude of the stream function, $k$ is the upslope wavenumber, $\sigma' = N_0 s_\beta$, $n_I = (k/2\Gamma)(s_{2\beta} - s_{2\alpha})$, $n_R = -(k/2\Gamma)(s_{2\alpha} + s_{2\beta})$ and $\Gamma = s_\beta^2 - s_\alpha^2$ (see Thorpe 1987, equation (20). This may be reduced to

$$\rho = (N_0^2 aks_\beta/g\sigma'\Gamma)[s_{\alpha+\beta}\cos(kx + n_R z) + s_{\alpha-\beta}\cos(kx + n_I z)]\sin\sigma' t. \tag{8}$$

When $\alpha$ is small, and $k = 2\pi/\lambda$ and (7) are used to simplify the equation, the density

perturbation is proportional to $3\cos k[x+(2z/z_\alpha)]+\cos k[x+(2z/3s_\alpha)]$. The vertical density structure, and hence the displacements, is dominated by the first term in this expression, which has a vertical wavelength of $\frac{2}{3}H$, twice the height of the overturning regions in figure 3. The subharmonic wave therefore sets the scale for the overturns, which appear at its standing wave 'crests', separated by distance $\lambda$, on one cycle of the forcing, and at the intermediate positions of the 'troughs', where the 'crests' subsequently occur on the next cycle. The position of the central overturn is dictated by symmetry along the tube, and the vertical scale of the overturns is set by the perturbation field of the subharmonic.

Static instability is observed to occur in the overturning eddy-like structures (e.g. figure 4*c*) resulting from the superposition of the primary oscillation (see in figure 2) and the parasitic subharmonic. We may estimate a Rayleigh number, $R$, of the overturn, and a parameter, $r$, such that the vertical density distribution in the overturning region is proportional to $(rKz-\sin Kz)$, where $K$ is a vertical wavenumber, following the method and analysis described by Thorpe (1994*b*) in a study of the stability of overturning standing internal waves. The Rayleigh number is equal to $gB_1h^3/(\mathscr{D}\nu)$, where $B_1$ is the positive density gradient at the centre of the unstably stratified region divided by the mean density, $\nu$ is the kinematic viscosity, and $\mathscr{D}$ is the diffusivity of salt in water. For the conditions of figure 4 and with a scale height, $h$, of $\frac{1}{3}H$, and taking $\nu = 1\times10^{-2}$ cm s$^{-1}$ and $\mathscr{D} = 1.4\times10^{-5}$ cm s$^{-1}$, we estimate that $R$ is equal to $2.1\times10^8$ and the parameter $r$ is 0.4. The Rayleigh number greatly exceeds the critical value of 56 at which instability is estimated to set in at this value of $r$ (see Thorpe 1994*a*, figure 7), so that the fluid in the overturned, statically unstable, region is predicted to be dynamically unstable. Growth rates of infinitesimal disturbances, $\gamma$, non-dimensionalized with the buoyancy frequency, $N$, increase as the Rayleigh number increases and as $r$ decreases. The non-dimensional growth rates, $\gamma_1 = \gamma N^{-1}$, at $R = 2.1\times10^8$ and $r = 0.4$, have been found using a series expansion (Thorpe, 1994*a*, §3.3) with truncation after 10 terms. The maximum growth rate, $\gamma_1 = 1.00\pm0.05$, corresponds to a dimensional growth rate, $\gamma$, of $1.12\pm0.06$ s$^{-1}$, and occurs at a disturbance wavenumber of $(7.2\pm0.2)/d_0$ directed *across* the tube, corresponding to a wavelength of $2.91\pm0.08$ cm. This implies a growth of the disturbance of 70–112 times in the 4 s period between figures 4(*b*) and 4(*d*), and gives e-folding rates 2.7 times the largest of those found in the experiments on overturning standing internal waves (Thorpe 1994*b*), where the corresponding values of $R$ and $r$ were $6.94\times10^7$ and 0.87, respectively. The validity of the theory is however in doubt, both because nonlinear effects were omitted and because the aspect ratio of the overturn is not small and, in particular, is much larger than that of the '$z$-shaped' isopycnal overturns in standing or progressive waves for which the theory is designed. The expectation of large growths rates is however consistent with the observed onset of mixing in these experiments.

## 4. Conclusion

McEwan & Robinson's (1975) study of small-amplitude parametric instability appears to be the only laboratory experiment, other than those on standing waves in which 'traumata' are observed (§1), in which the instability has been reported. In the present experiments, the vertical scale of the parasitic waves is larger than that of the 'traumata' reported by McEwan & Robinson, the scale of the overturning region of statically unstable fluid becoming comparable with the depth of the tube, and there is clear evidence of the development of convective motions and mixing. The overturning structure contrasts with the horizontally elongated z-shaped isopycnal folding in thin

layers found in internal waves in earlier tilted-tube experiments (Thorpe 1978*a*, *b*, 1981), and in particular with those described by Thorpe (1994*b*). The experiments provide direct evidence that parametric instability can indeed lead to convective motions and to mixing. The vertical scale selected by the parametric instability, both as here in confined regions, and in the natural environment, remains to be fully explained.

The experiments were made at the Centre for Water Research at the University of Western Australia during a period of study leave in 1992. I am grateful to Mr John Devill and to Mr Bill Deugh for their expert construction of apparatus, to Mr Seng Giap Teoh, Mrs Silvia Bruno and to my wife, Daph, for their help in recording the results, and to the CWR and the Royal Society for financial support which made the visit possible.

## REFERENCES

DRAZIN, P. G. 1977 On the instability of an internal gravity wave. *Proc. R. Soc. Lond.* A **356**, 411–432.

IVEY, G. N. & NOKES, R. I. 1989 Vertical mixing due to the breaking of critical internal waves on sloping boundaries. *J. Fluid Mech.* **204**, 479–500.

KLOSTERMEYER, J. 1982 On parametric instabilities of finite-amplitude internal gravity waves. *J. Fluid Mech.* **119**, 367–377.

KLOSTERMEYER, J. 1983 Parametric instabilities of internal gravity waves in Boussinesq fluids with large Reynolds numbers. *Geophys. Astrophys. Fluid Dyn.* **26**, 85–105.

KLOSTERMEYER, J. 1984 Observations indicating parametric instabilities in internal gravity waves at thermospheric heights. *Geophys. Astrophys. Fluid Dyn.* **29**, 117–138.

KLOSTERMEYER, J. 1990 On the role of parametric instability of internal gravity waves in atmospheric radar observations. *Radio Sci.* **25**, 983–995.

MCEWAN, A. D. 1971 Degeneration of resonantly excited standing internal gravity waves. *J. Fluid Mech.* **50**, 431–448.

MCEWAN, A. D. 1973 Interactions between internal gravity waves and their traumatic effect on a continuous stratification. *Boundary-Layer Met.* **5**, 159–175.

MCEWAN, A. D. & ROBINSON, R. M. 1975 Parametric instability of internal gravity waves. *J. Fluid Mech.* **67**, 667–687.

MIED, R. P. 1976 The occurrence of parametric instability in finite-amplitude internal gravity waves. *J. Fluid Mech.* **78**, 763–784.

PHILLIPS, O. M. 1966 *The Dynamics of the Upper Ocean.* Cambridge University Press.

TAYLOR, J. 1992 The energetics of breaking events in a resonantly forced internal wave field *J. Fluid Mech.* **239**, 309–340.

THORPE, S. A. 1978*a* On the shape and breaking of finite-amplitude internal gravity waves in a shear flow. *J. Fluid Mech.* **85**, 7–31.

THORPE, S. A. 1978*b* On internal gravity waves in an accelerating shear flow. *J. Fluid Mech.* **88**, 623–639.

THORPE, S. A. 1981 An experimental study of critical layers. *J. Fluid Mech.* **103**, 321–344.

THORPE, S. A. 1987 On the reflection of a train of finite amplitude internal gravity waves from a uniform slope. *J. Fluid Mech.* **178**, 185–196.

THORPE, S. A. 1994*a* The stability of statically unstable layers. *J. Fluid Mech.* **260**, 315–331.

THORPE, S. A. 1994*b* Statically unstable layers produced by overturning internal gravity waves. *J. Fluid Mech.* **260**, 333–350.